

JAPAN ANNUAL REVIEWS IN ELECTRONICS
COMPUTERS AND & TELECOMMUNICATIONS

Vol. 5

OPTICAL DEVICES & FIBERS

Editor Y. SUEMATSU

JAPAN ANNUAL REVIEWS IN ELECTRONICS, COMPUTERS & TELECOMMUNICATIONS

Vol. 5

OPTICAL DEVICES & FIBERS



OHM

Tokyo • Osaka • Kyoto



NORTH-HOLLAND

Amsterdam • New York • Oxford



OHMSHA, LTD. and



NORTH-HOLLAND PUBLISHING COMPANY

Copyright © 1983 by OHMSHA, LTD.

ISSN 0167-50036

Co-published by
OHMSHA, LTD.

1-3 Kanda Nishiki-cho, Chiyoda-ku, Tokyo 101, Japan

Sole distributors for Japan

and

NORTH-HOLLAND PUBLISHING COMPANY

Molenwerf 1, 1014 AG, Amsterdam, The Netherlands

Sole distributors for outside Japan

All rights reserved. No part of this publication may be reproduced, stored in a retrieval system, or transmitted in any form or by any means, electronic or mechanical, photocopy, recording, or otherwise, without the prior written permission of the publishers.

Special regulations for readers in the U.S.A.—This journal has been registered with the Copyright Clearance Center, Inc. Consent is given for copying of articles for personal or internal use, or for the personal use of specific clients. This consent is given on the condition that the copier pays through the Center the per copy fee stated in the code on the first page of each article for copying beyond that permitted by Sections 107 or 108 of the U.S. Copyright Law. The appropriate fee should be forwarded with a copy of the first page of the article to the Copyright Clearance Center, Inc., 21 Congress Street, Salem, MA 01970, U.S.A. If no code appears in an article, the author has not given broad consent to copy and permission to copy must be obtained directly from the author. All articles published prior to 1981 may be copied for a per-copy fee of US \$2.25, also payable through the Center. (N.B. For review journals this fee is \$0.20 per copy per page.) This consent does not extend to other kinds of copying, such as for general distribution, resale, advertising and promotion purposes, or for creating new collective works. Special written permission must be obtained from the publisher for such copying.

Special regulations for authors in the U.S.A.—Upon acceptance of an article to the journal, the author(s) will be asked to transfer copyright of the article to the publisher. This transfer will ensure the widest possible dissemination of information under the U.S. Copyright Law.

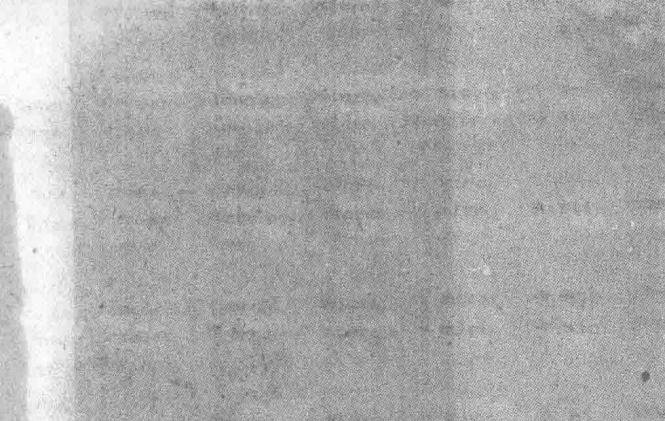
Printed in Japan

NORTH-HOLLAND


Amsterdam · New York · Oxford

OHM

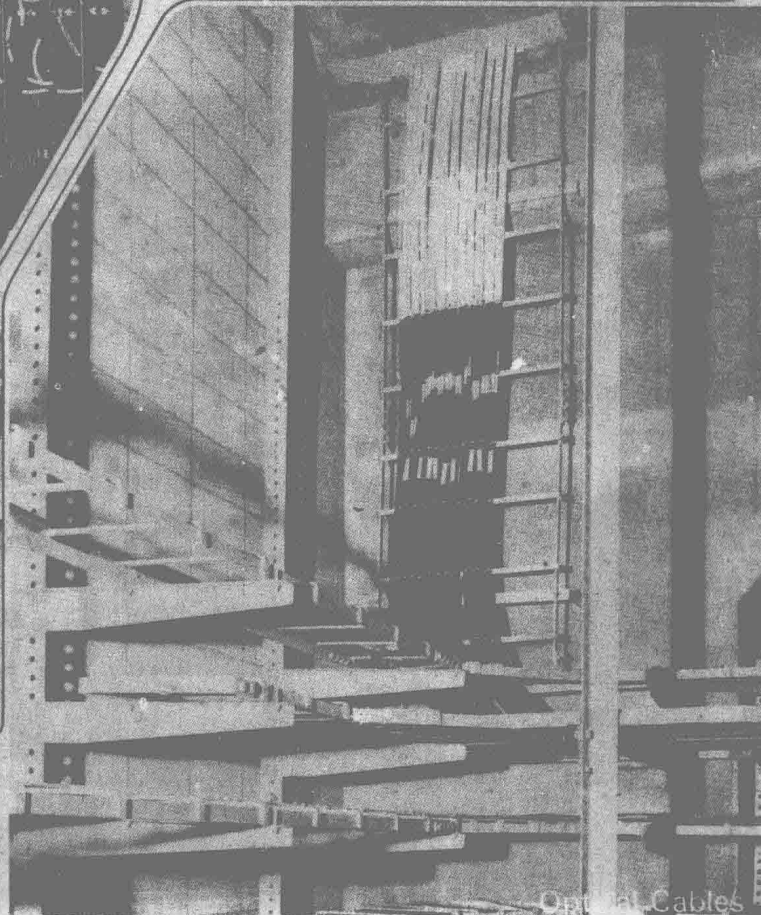
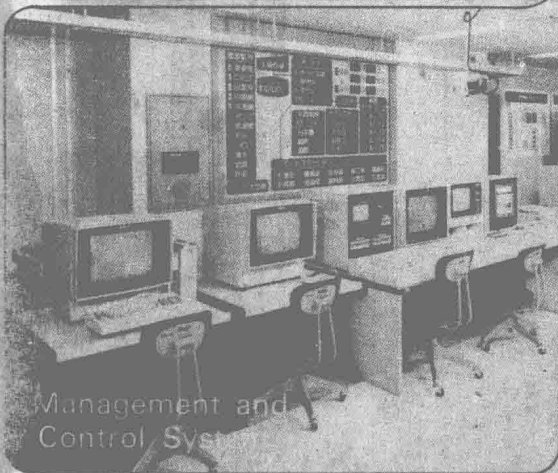
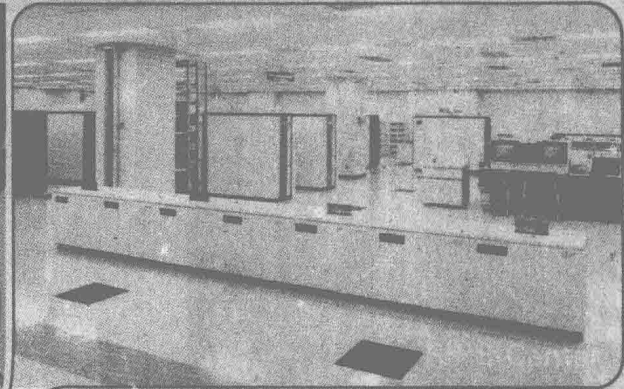
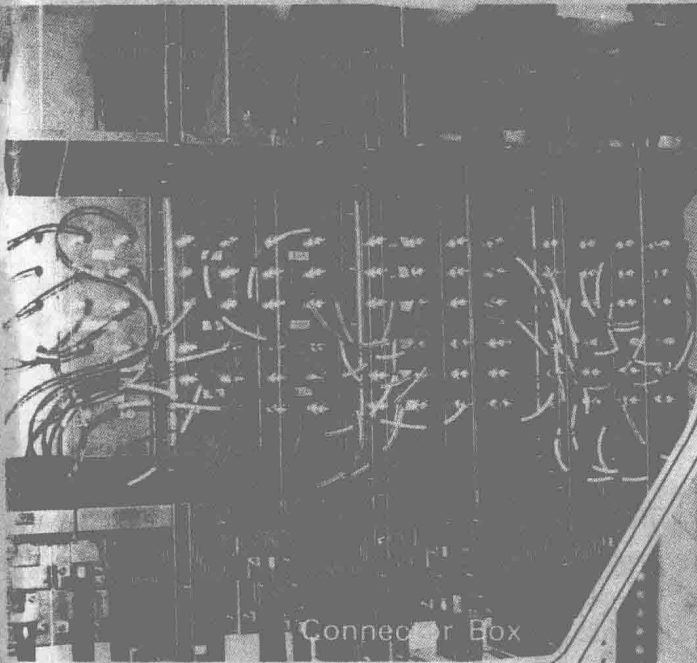
Tokyo · Osaka · Kyoto



▲ Real Images Made by a Planar
Microlens Array

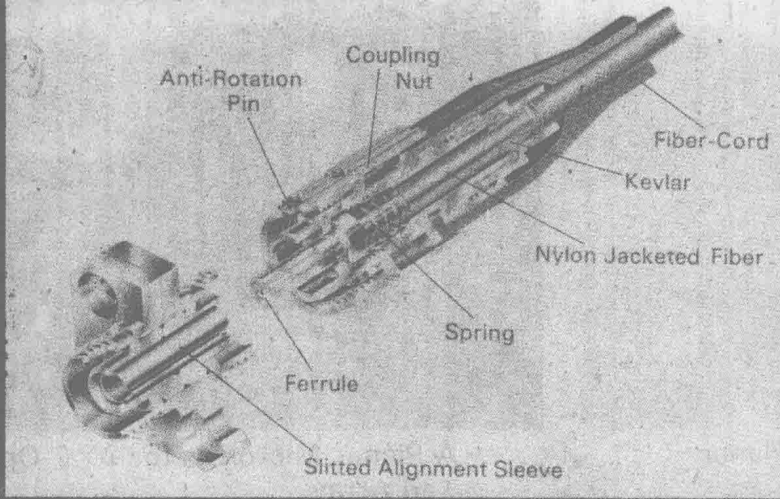


▲ A Planar Microlens for 2×2 Optical
Tap Array
(See Section 2.4)



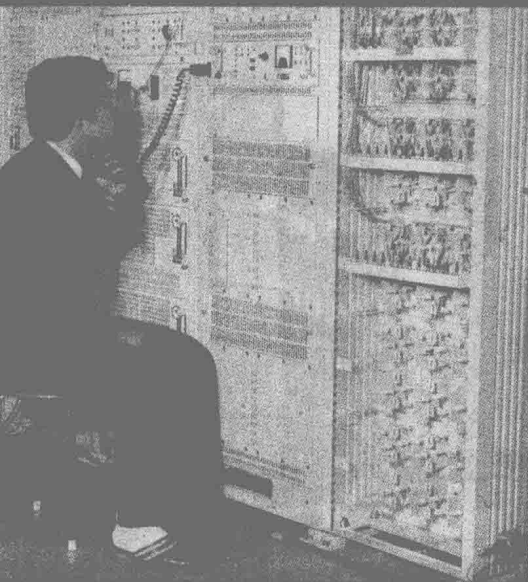
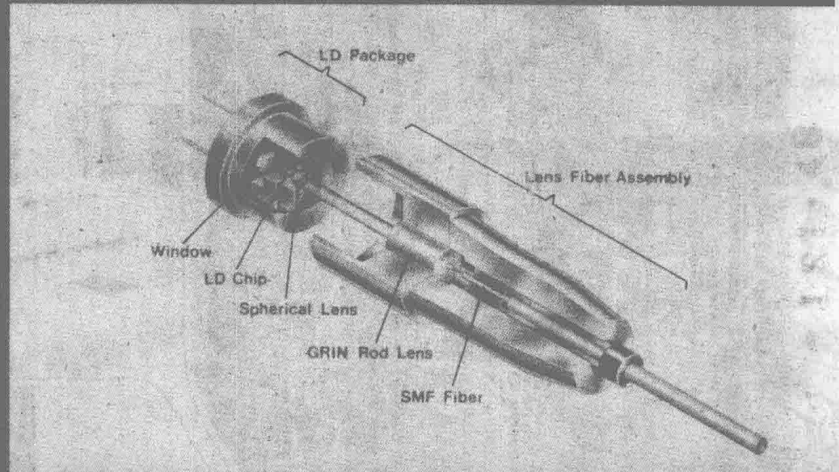
▲ Research Information Processing
System (RIPS Network)

(See Section 4.1)



◀ Single-Mode Fiber FA (Field Assembly) Connector

▶ Laser Diode Module for Single-Mode Fibers



▲ Repeater Test for the F-400M System



▲ Transmission Equipment of the F-400M System

(See Section 4.4)

Preface

The recent studies of lightwave devices and optical fibers as well as their possible applications are given in this JARECT Vol. 5 to introduce the activities of the leading Japanese scientists and experts, followed after the previous edition of 1982. Very rapid and significant developments are performed in the field of opto-electronics, especially for the lightwave communications. Contents of this volume is written for scientists and engineers of laboratories and manufacturing industries as well as users in relevant industries, and graduate students.

The contents well cover whole area of optical communications and components for opto-electronics.

Different aspects of topics which are not included in the 1982 edition are discussed in this volume. Altogether of twenty-two subjects are distributed into four sections, namely, Device, Component, Fiber, and System. The authors of those subjects are leading experts selected by the members of the editorial and planning committee according to suggestions of the members of the advisory committee.

In the Device section, recently developed following seven subjects are discussed: the devices for coherent systems, the visible semiconductor laser, the fabrication of AlGaAs/GaAs lasers by metal-organic-chemical-vapor-deposition (MOCVD), the germanium avalanche photo-diodes for long-wavelength optical communications, the temperature characteristics of InGaAsP long-wavelength light sources, the $1.55\mu\text{m}$ long-wavelength single-mode lasers, and the quality control of semiconductor laser at the production stage.

In the Component section, following six subjects of interest are discussed: the optical multi- and demultiplexer for the wavelength division multiplexed communication, the integrated optical branching filter of three-dimensional waveguide-type, the distributed-index planar microlens, the gradient-index rod lenses, and the optical waveguide-type lenses, switches and integrated optics.

In the Fiber section, discussions are concentrated to following five subjects: the infrared optical fiber, the temperature characteristics of loss mechanism for optical cable, the optical fiber splicing, the measurement of index profiles of fibers and preforms, and the bandwidth estimation of multiplexed multimode fibers.

In the System section, following four subjects are discussed: the research

PREFACE

information processing system called RIPS network, the wavelength-division-multiplexing optical transmission, the evaluation of laser mode-partition-noise in optical fiber transmission, and the long distance fiber transmission.

The editor acknowledges the numerous efforts of members of the editorial and planning committee and members of the advisory committee. He also appreciates the efforts of Messrs. S. Sato, M. Mori and T. Yamanouchi of Ohmsha, Ltd.

Yasuharu Suematsu
Editor

Tokyo, Japan
January 1983

Contents

PREFACE

Chapter 1	DEVICE	1
1.1	Optical Devices for Coherent Transmission Systems	2
	<i>T. Kimura, Y. Yamamoto; Musashino Electrical Communication Laboratory, NTT</i>	
1.2	Fabrication of GaAlAs/GaAs Visible TS Lasers	23
	<i>M. Wada, K. Itoh, T. Sugino, H. Shimizu, I. Teramoto; Matsushita Electronics Corporation</i>	
1.3	AlGaAs/GaAs Laser Diodes Grown by MOCVD — A Review	35
	<i>Y. Mori, N. Watanabe; Sony Corporation Research Center</i>	
1.4	Germanium Avalanche Photodiodes for Optical Fiber Communication Systems	48
	<i>T. Kaneda; Fujitsu Laboratories Ltd.</i>	
	<i>H. Kanbe; Musashino Electrical Communication Laboratory, NTT</i>	
1.5	Temperature Characteristics of InGaAsP Laser Diodes and Light Emitting Diodes	59
	<i>T. Kamiya, N. Kamata; The University of Tokyo</i>	
1.6	1.55 μm Wavelength InGaAsP/InP Single-Mode Lasers	70
	<i>T. Ikegami; Musashino Electrical Communication Laboratory, NTT</i>	
	<i>T. Yamamoto; KDD Co., Ltd.</i>	
1.7	Quality Control of AlGaAs TJS Laser Diodes at an Early Production Stage	81
	<i>S. Takamiya; Mitsubishi Electric Corp.</i>	
Chapter 2	COMPONENT	95
2.1	Optical Multiplexer and Demultiplexer	96
	<i>R. Watanabe; Yokosuka Electrical Communication Laboratory, NTT</i>	
2.2	Integrated Optical Branching Filter and Delay Equalizer Consisting of Three-Dimensional Waveguide and Its Nonradiative Condition	114
	<i>K. Furuya, Y. Suematsu, S. Sugou; Tokyo Institute of Technology</i>	

CONTENTS

2.3	Optical Isolator for 1.2 ~ 1.7 μm Wavelength	129
	<i>T. Aoyama, T. Hibiya; Nippon Electric Co., Ltd.</i>	
2.4	Distributed-Index Planar Microlens	142
	<i>K. Iga, M. Oikawa; Tokyo Institute of Technology</i>	
2.5	Current Status of Gradient-Index Rod Lenses	151
	<i>I. Kitano; Nippon Sheet Glass Co., Ltd.</i>	
2.6	Optical Waveguide Lenses, Switches and Integrated Circuits	167
	<i>H. Nishihara, M. Haruna, T. Suhara; Osaka University</i>	
Chapter 3	FIBER	181
3.1	Infrared Optical Fibers	182
	<i>S. Yoshida, H. Murata; The Furukawa Electric Co., Ltd.</i>	
3.2	Loss Increase Mechanism of Optical Cable in Wide Temperature Range ...	196
	<i>R. Yamauchi, K. Inada; Fujikura Ltd.</i>	
3.3	Optical Fiber Splicing	209
	<i>M. Hoshikawa, Y. Toda; Sumitomo Electric Industries, Ltd.</i>	
3.4	Measurement of Refractive-Index Profiles of Optical Fibers and Preforms	219
	<i>T. Okoshi, K. Hotate; The University of Tokyo</i>	
3.5	Bandwidth Characteristics of Multispliced Graded-Index Fibers	235
	<i>T. Matsumoto; Yokosuka Electrical Communication Laboratory, NTT</i>	
Chapter 4	SYSTEM	249
4.1	RIPS Network — Research Information Processing System —	250
	<i>K. Yada; Electrotechnical Laboratory</i> <i>T. Ochiai, M. Honda; Fujitsu Ltd.</i>	
4.2	Fiber-Optic Wavelength-Division-Multiplexing Technology and Its Application	268
	<i>K. Nosu; Yokosuka Electrical Communication Laboratory, NTT</i>	
4.3	Laser Partition Noise Evaluation for Optical Fiber Transmission	291
	<i>Y. Okano, K. Nakagawa, T. Ito; Yokosuka Electrical Communication Laboratory, NTT</i>	
4.4	High Quality Long Distance Fiber Transmission	303
	<i>S. Shinohara, T. Ito; Yokosuka Electrical Communication Laboratory, NTT</i>	
Authors' Profile		315

Chapter 1 DEVICE

Chapter 1 DEVICE

1.1 Optical Devices for Coherent Transmission Systems

Tatsuya KIMURA* and Yoshihisa YAMAMOTO*

Abstract

Constituent devices and related technologies of coherent optical fiber transmission systems are reviewed. Frequency modulation noise and spectral linewidth in a semiconductor laser and its reduction with external grating feedback are studied theoretically and experimentally. Direct observation of Lorentzian lineshape, comparison of theoretical and experimental linewidth (and FM noise spectrum) and linewidth reduction to less than 40 kHz with an external grating feedback are described.

Direct frequency modulation in a semiconductor laser by means of injection current modulation were investigated. It is shown that temperature change is responsible for frequency modulation at low modulation frequency and that carrier density change is responsible at high modulation frequency. Frequency deviation of 100 MHz to 1 GHz is obtained by modulation current of only 1% of the oscillation threshold current. Theoretical analyses, using a rate equation with lateral carrier and optical field distribution and a dynamic thermal equation, are in good agreement with experimental results.

Heterodyne detection of optical FSK signal and local oscillator frequency stabilization were performed. IF frequency stabilization by means of drive current feedback and successful demodulation of 100 Mbit/s FSK signal are presented.

Theoretical and experimental results on signal gain, frequency bandwidth and saturation output power of Fabry-Perot resonant type and traveling-wave type semiconductor laser amplifiers are described. 20~30 dB signal gain, 2~10 GHz frequency bandwidth and -10 dBm to -5 dBm saturation output power were obtained in AlGaAs laser amplifiers. Noise characteristics and signal-to-noise ratio were analyzed by the quantum mechanical rate equation and by the density matrix master equation, which are found to agree with experimental noise characteristics.

Signal gain, locking bandwidth and FM signal amplification properties of an injection locked semiconductor laser were measured for AlGaAs laser and analyzed by van der Pol equation with input signal term.

The applications of these amplifiers to optical repeaters in a coherent transmission system are finally discussed.

* Musashino Electrical Communication Laboratory, Nippon Telegraph and Telephone Public Corporation, Musashino 180.

1.1.1 Introduction

Optical fiber transmission systems developed so far have employed optical energy transmission with an intensity modulation-direct detection scheme. Improved system performance is expected in coherent optical transmission systems utilizing amplitude or angle modulation of coherent laser wave and optical heterodyne (or homodyne) detection.^{1,2)} Coherent optical transmission was studied for a space communication system using frequency stabilized He-Ne laser or CO₂ laser,³⁾ but has not been applied to a fiber communication system using semiconductor lasers, due to their insufficient frequency stability and coherence.

The initial optical FSK modulation-demodulation experiment, using semiconductor lasers, has been successfully demonstrated.^{4,5)} It indicated the feasibility that a coherent optical fiber transmission system could be realized by compact and stable constituent devices.

Basic configuration for a coherent transmission system is shown in Fig. 1.1.1. The transmitter consists of a frequency stabilized laser oscillator, an optical phase or frequency modulator, an optical post-amplifier and optical isolators between them. Receiver consists of a local laser oscillator, an optical duplexer combining signal and local waves, a photodetector as a mixer and electronic demodulation circuitry. Optical fiber is devised for maintaining the polarization state of signal wave and may be incorporated with a polarization control device. An optical amplifier repeater can be optionally used to compensate for fiber loss and to expand electronic regenerative repeater spacing.

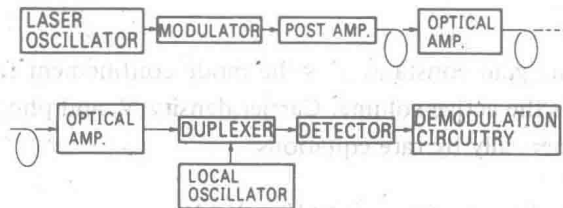


Fig. 1.1.1 Basic configuration of coherent optical fiber transmission system.

Characteristics of various constituent devices and related technologies developed so far are reviewed in this article. System considerations, such as required device properties and expected system performance, have already been reported in previous publications^{1,2)} and are not reported here.

1.1.2 Frequency Modulation Noise and Spectral Linewidth in a Semiconductor Laser^{11,15,16,26)}

Quantum phase noise (frequency modulation noise), caused by spontaneous emission coupled to a lasing mode, is important in coherent optical FSK and PSK systems, since it directly affects a signal-to-noise ratio.²⁾

Frequency modulation noise in a laser is characterized by an oscillation power spectrum or by a frequency modulation noise spectrum. An oscillation power spectrum $W_e(\nu)$ is experimentally observed by mixing the test laser output with frequency stabilized reference laser

output and displaying the beat tone on a spectrum analyzer. It has a Lorentzian form

$$W_e(\nu) = 1/[1 + 4\{(\nu - \nu_0)^2 / \Delta\nu_{1/2}^2\}] \quad (1.1.1)$$

where ν_0 is oscillation center frequency and $\Delta\nu_{1/2}$ is full linewidth at half maximum. A frequency modulation noise spectrum $W_{\delta F}(f)$, on the other hand, is experimentally observed by displaying the frequency discriminator output of beat tone mentioned above on the spectrum analyzer. It is given by

$$W_{\delta F}(f) = K_d^2 \Delta\nu_{1/2} g(\nu_0 + f) / g(\nu_0) \quad (1.1.2)$$

where K_d is the frequency discriminator constant in V/Hz and $g(\nu)$ is the transition line shape function. Although the frequency modulation noise spectrum $W_{\delta F}(f)$ is directly related to signal-to-noise ratio in the FSK system, it had not been mentioned until 1974⁶⁾ and has attracted little attention so far. From Eq. (1.1.2), the cutoff frequency for $W_{\delta F}(f)$ is in the range of 10^{12} Hz to 10^{13} Hz for a semiconductor laser, which is quite different from an amplitude modulation noise spectrum, which has several GHz-cutoff frequency.

Linewidth $\Delta\nu_{1/2}$ is determined by the ratio of spontaneous noise photon coupling to lasing mode $\beta N_e / \tau_s$ to signal photon numbers N_p ^{7,8)}:

$$\Delta\nu_{1/2} = \beta N_e / (4\pi \tau_s N_p) \quad (1.1.3)$$

where τ_s is spontaneous lifetime and β is the factor of spontaneous emission coupled to a lasing mode,

$$\beta = \Gamma A \tau_s / V \quad (1.1.4)$$

Here, A is the differential gain constant, Γ is the mode confinement factor, τ_s is the spontaneous life time and V is the active volume. Carrier density N_e and photon density N_p in Eq. (1.1.3) are obtained numerically by rate equations:

$$\frac{dN_e}{dt} = J / (ed) - N_e / \tau_s - A \Gamma (N_e - N_0) N_p \quad (1.1.5)$$

$$\frac{dN_p}{dt} = A \Gamma (N_e - N_0) N_p + \beta N_e / \tau_s - N_p / \tau_p \quad (1.1.6)$$

Gain saturation effect plays an important role in regard to FM noise property as well as AM noise suppression, which is implicitly included in the rate Eqs. (1.1.5) and (1.1.6).

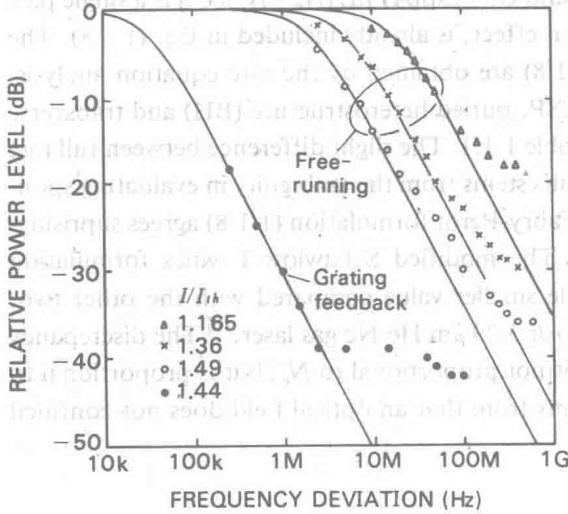
Direct observations of Lorentzian line shapes have been reported for $10.6 \mu\text{m}$ $\text{Pb}_{0.88}\text{Sn}_{0.12}\text{Te}$ diode laser,⁹⁾ $3.39 \mu\text{m}$ He-Ne laser¹⁰⁾ and $0.84 \mu\text{m}$ AlGaAs laser.¹¹⁾ Figure 1.1.2 shows the oscillation power spectrum for channeled-substrate-planar (CSP) AlGaAs laser, which was measured by optical heterodyne detection using two distinct AlGaAs lasers.¹¹⁾ The experimental results are in good agreement with the theoretical Lorentzian line shape shown by solid lines except for the noise floor due to receiver thermal noise. Theoretical and experimental spectral linewidth $\Delta\nu_{1/2}$ values for a CSP laser are shown in Fig. 1.1.2(d) as a function of pumping level $I/I_{th} - 1$.

The linewidth is conventionally calculated by the modified Schawlow-Townes formula-

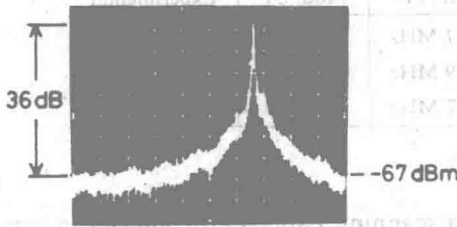
tion for gas and solid state lasers

$$\Delta\nu_{1/2} = \pi h\nu (\Delta\nu_c)^2 n_{sp} / P_0 \quad (1.1.7)$$

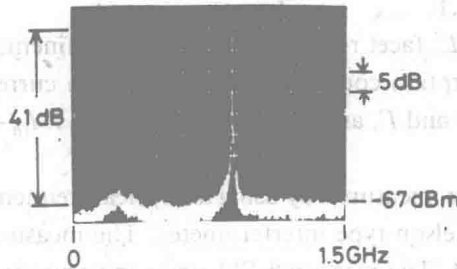
where $\Delta\nu_c = 1/(2\pi\tau_p)$ is cold cavity linewidth, $\tau_p = \left[\frac{c}{n} \left(\alpha + \frac{1}{L} \ln \frac{1}{R} \right) \right]^{-1}$ is photon lifetime, $P_0 =$



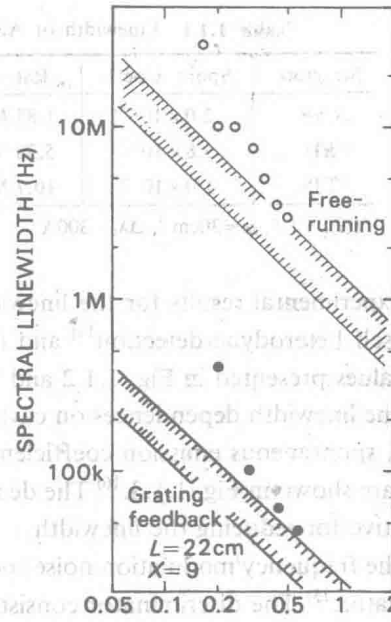
(a)



(b)



(c)



(d)

Fig. 1.1.2 (a) Oscillation line shapes for solitary and external grating controlled AlGaAs lasers. Solid lines denote theoretical Lorentzian line shape.

(b) Beat note spectrum between two solitary AlGaAs lasers at $I/I_{th} = 1.49$.

(c) Beat note spectrum between two external grating controlled AlGaAs lasers at $I/I_{th} = 1.44$.

(d) Spectral linewidth vs. injection current for solitary and external grating controlled AlGaAs lasers. [after S. Saito et al.¹¹⁾]

$h\nu N_p V / (\tau_p \Gamma)$ is total emitted power including that going to a loss and n_{sp} is a factor determined by population inversion. The finesse of active Fabry-Perot cavity also corresponds to the spectral linewidth

$$\Delta\nu_{1/2} = c(1 - RG_s) / [4\pi nL\sqrt{RG_s}] \quad (1.1.8)$$

where L is cavity length, R is facet reflectivity and $G_s = \exp[A\Gamma nL(N_e - N_o)/C]$ is a single pass gain. The factor of two, due to gain saturation effect, is already included in Eq. (1.1.8). The values of P_0 in Eq. (1.1.7) and G_s in Eq. (1.1.8) are obtained by the rate equation analysis. Theoretical and experimental linewidths for CSP, buried heterostructure (BH) and transverse junction stripe (TJS) lasers are compared in Table 1.1.1. The slight difference between full rate equation analysis (1.1.3) and experimental results stems from the ambiguity in evaluating spontaneous emission coefficient β . Simple active Fabry-Perot formulation (1.1.8) agrees surprisingly well with the full rate equation analysis. The modified Schawlow-Townes formulation (1.1.7), however, gives an order of magnitude smaller value compared with the other two, though it can accurately predict the linewidth for $3.39 \mu\text{m}$ He-Ne gas laser.¹⁰⁾ The discrepancy stems from that a stimulated gain coefficient is not proportional to N_e , but is proportional to $N_e - N_o$ in a semiconductor laser and also stems from that an optical field does not confined completely inside an active region.

Table 1.1.1 Linewidth of AlGaAs lasers calculated by three models.

Structure	Spont. Coeff.	Rate Eq.	Act. FP	Mod. ST	Experimental
CSP	2.0×10^{-5}	1.85 MHz	1.87 MHz	269 kHz	2 MHz
BH	5.8×10^{-5}	5.38 MHz	5.39 MHz	404 kHz	—
TJS	1.0×10^{-4}	10.7 MHz	10.7 MHz	785 kHz	6.4 MHz

$$I/I_{th} = 1.5, \alpha = 30\text{cm}^{-1}, \Delta\lambda_s = 300\text{\AA}$$

Experimental results for the linewidth with a scanning Fabry-Perot interferometer,¹²⁾ delayed self heterodyne detection¹³⁾ and interferometric FM-AM noise conversion^{14,15)} gives similar values presented in Fig. 1.1.2 and Table 1.1.1.

The linewidth dependences on cavity length L , facet reflectivity R , mode confinement factor Γ , spontaneous emission coefficient β , absorption coefficient α and injection current $I/I_{th} - 1$ are shown in Fig. 1.1.3.¹⁶⁾ The decrease in β and Γ , and the increase in L and $I/I_{th} - 1$ are effective for reducing the linewidth.

The frequency modulation noise spectrum was measured by using an optical frequency discriminator.¹⁵⁾ The discriminator consists of Michelson type interferometer. The measured frequency deviation spectrum is shown in Fig. 1.1.4. The measured FM noise spectrum is in agreement with theoretical results Eq. (1.1.2). Here, the decrease in FM noise spectrum at higher frequency than 1 GHz stems from the optical discriminator cut-off frequency.

Baseband signal to noise ratio in the optical FSK system is degraded by quantum FM noise, as follows:

$$S/N = \Delta f_s^2 / [(\Delta\nu_{1/2}^T + \Delta\nu_{1/2}^{LO})B_0] \quad (1.1.9)$$

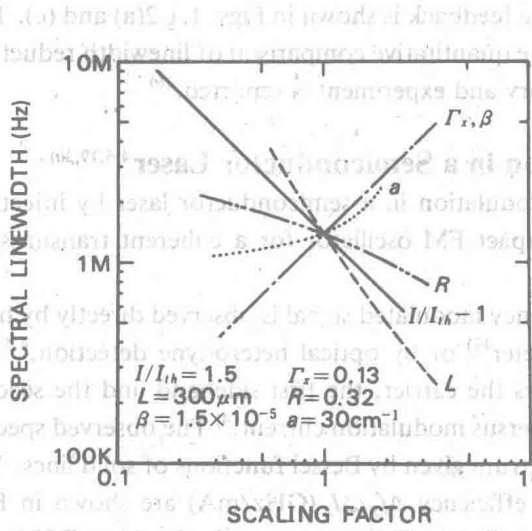


Fig. 1.1.3 Spectral linewidth in AlGaAs laser as a function of pumping level $I/I_{th}-1$, cavity length L , spontaneous emission coefficient β , mode confinement factor Γ , facet reflectivity R and absorption loss α .

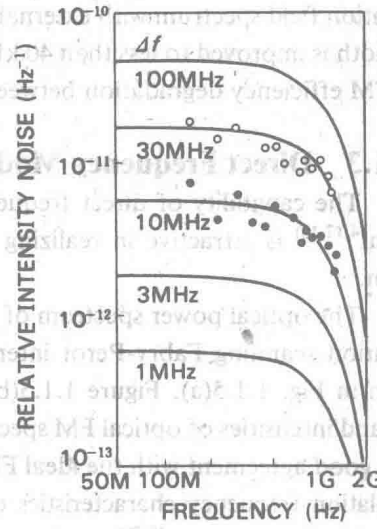


Fig. 1.1.4 Frequency modulation noise spectrum for AlGaAs laser measured by FM-AM conversion with optical frequency discriminator. Delay time of Michelson interferometer is 400 picoseconds. [after Y. Yamamoto et al.¹⁵⁾]

where Δf_s is frequency shift between mark and space signals and B_0 is baseband filter bandwidth. For 400 Mbit/s FSK system employing $\Delta f_s = 200$ MHz, $(\Delta\nu_{1/2}^T + \Delta\nu_{1/2}^{LO})$ should be less than 100 kHz to achieve $S/N \geq 30$ dB.

The external grating feedback to a semiconductor laser is useful for oscillating longitudinal mode selection and wide range of frequency tunability over 1 THz.^{24,25)} It is expected to be effective to suppress an FM noise at some expense of mechanical stability and direct frequency modulation capability.

The oscillation power spectrum is modified from simple Lorentzian Eq. (1.1.1) to

$$W_e(\nu) = [1 + 4 \{ (1 + X \sin \Delta\omega\tau_2 / \Delta\omega\tau_2)^2 + X^2 (1 - \cos \Delta\omega\tau_2)^2 / (\Delta\omega\tau_2)^2 \} \times (\nu - \nu_0)^2 / \Delta\nu_{SL}^2]^{-1} \quad (\Delta\omega = 2\pi(\nu - \nu_0)) \quad (1.1.10)$$

where $\Delta\nu_{SL}$ is a solitary diode laser linewidth. Parameter X is an important measure of the feedback effect, which is given by

$$X = (1 - R)(R_{ex} / R)^{1/2} \tau_2 / \tau_1 \quad (1.1.11)$$

where $1/\tau_1$ is a solitary diode laser axial mode separation, $1/\tau_2$ is an external cavity axial mode separation and R_{ex} is effective reflectivity of external grating, including diffraction loss. The linewidth can be improved with employing external cavity structure by a factor $(1 + X)^2$. The

oscillation field spectrum with external grating feedback is shown in Figs. 1.1.2(a) and (c). The linewidth is improved to less than 40 kHz. The quantitative comparison of linewidth reduction and FM efficiency degradation between theory and experiment is reported.²⁶⁾

1.1.3 Direct Frequency Modulation in a Semiconductor Laser^{4,5,19,20)}

The capability of direct frequency modulation in a semiconductor laser by injection current^{4,17,18)} is attractive in realizing a compact FM oscillator for a coherent transmission system.

The optical power spectrum of frequency modulated signal is observed directly by high resolution scanning Fabry-Perot interferometer¹⁹⁾ or by optical heterodyne detection,^{4,5)} as shown in Fig. 1.1.5(a). Figure 1.1.5(b) shows the carrier, the first sideband and the second sideband intensities of optical FM spectrum versus modulation current.⁴⁾ The observed spectra are in good agreement with the ideal FM spectrum given by Bessel functions of solid lines. The modulation frequency characteristics of FM efficiency $\Delta f_s / \Delta I_m$ (GHz/mA) are shown in Fig. 1.1.5(c) for a CSP laser.^{19,20)} Similar but more efficient FM response is obtained in a TJS laser. BH laser, however, exhibits the steep decrease in the FM response at about 100 MHz.²⁰⁾ The frequency shift of 200 MHz to 5 GHz is obtained by 1 mA modulation current, which corresponds to 1~3% of oscillation threshold current. Spurious intensity modulation, accompanied with the frequency modulation, is within several percent, which can be easily eliminated by a limiting device, such as injection locked post-amplifiers.

The solid lines in Fig. 1.1.5(c) represent theoretical FM efficiency caused by the active layer refractive-index change due to carrier density modulation, which is calculated by

$$\Delta f_s / f_0 = (C_{BB} + C_{FC}) \Gamma \int \Delta N_e(x) |E(x)|^2 dx / \bar{n} \quad (1.1.12)$$

where C_{BB} is a coefficient of refractive-index change due to anomalous dispersion accompanied with band-to-band transition,²¹⁾ C_{FC} is that due to free carrier plasma effect,²²⁾ $E(x)$ is normalized optical field and $N_e(x)$ is distribution of carrier density modulation along the lateral direction, which is numerically obtained by the rate equation with lateral carrier and optical field distribution,

$$\frac{dN_e(x)}{dt} = J(x) / (ed) - N_e(x) / \tau_s + L_D^2 \frac{d^2 N_e(x)}{dx^2} / \tau_s - A \Gamma [N_e(x) - N_0] S(x) \quad (1.1.13)$$

$$\frac{dS(x)}{dt} = A \Gamma [N_e(x) - N_0] S(x) + \beta N_e(x) / \tau_s - N_e(x) / \tau_p \quad (1.1.14)$$

Here L_D is diffusion length and $S(x)$ is photon density in the active layer. The resonant peak in FM efficiency above 1 GHz stems from the relaxation oscillation, which coincides to the peak in intensity modulation.

In a BH laser, carrier and optical field are well confined within the optical core region. Therefore, the lasing field is high enough to clamp the quasi-Fermi level (carrier density). This is the reason why FM efficiency is small in low modulation frequency range in BH laser. The clamp of quasi-Fermi level by the lasing field becomes incomplete with increasing the modulation frequency, because build up of optical field is delayed with respect to the carrier modulation.